

Negative index bulk metamaterial at terahertz frequencies

Oliver Paul¹, Christian Imhof², Benjamin Reinhard¹, Remigius Zengerle² and René Beigang^{1,3}

¹Department of Physics, University of Kaiserslautern, Germany

²Department of Electrical and Computer Engineering, University of Kaiserslautern, Germany

³Fraunhofer Institute for Physical Measurement Techniques IPM, Freiburg, Germany

Oliver.Pa@gmx.de

Abstract: We present a bulk metamaterial with negative refractive index in the terahertz frequency range. The structure is composed of pairs of metallic crosses embedded in Benzocyclobutene (BCB). The design is specifically chosen to provide a low-loss, free-standing material which operates under normal incidence and independently of the polarization of the incident radiation. These qualities allow the fabrication of 3D structures by mechanical stacking of multiple thin films.

© 2008 Optical Society of America

OCIS codes: (160.3918) Metamaterials; (350.3618) Lefthanded materials; (300.6495) THz spectroscopy; (220.4000) Microstructure fabrication

References

1. R. A. Silin, "Possibility of creating plane-parallel lenses," *Opt. Spectrosc.* **44**, 189–191 (1978).
2. J. B. Pendry, "Negative Refraction Makes a Perfect Lens," *Phys. Rev. Lett.* **85**, 3966–3969 (2000).
3. V. A. Fedotov, P. L. Mladyonov, S. L. Prosvirnin, and N. I. Zheludev, "Planar electromagnetic metamaterial with a fish scale structure," *Phys. Rev. E* **72**, 056,613 (2005).
4. J. B. Pendry, D. Schurig, and D. R. Smith, "Controlling Electromagnetic Fields," *Science* **312**, 1780–1782 (2006).
5. U. Leonhardt, "Optical Conformal Mapping," *Science* **312**, 1777–1780 (2006).
6. D. Schurig, J. J. Mock, B. J. Justice, S. A. Cummer, J. B. Pendry, A. F. Starr, and D. R. Smith, "Metamaterial Electromagnetic Cloak at Microwave Frequencies," *Science* **312**, 977–980 (2006).
7. A. V. Rogacheva, V. A. Fedotov, A. S. Schwanecke, and N. I. Zheludev, "Giant Gyrotropy due to Electromagnetic-Field Coupling in a Bilayered Chiral Structure," *Phys. Rev. Lett.* **97**, 177,401 (2006).
8. Y. Svirko, N. Zheludev, and M. Osipov, "Layered chiral metallic microstructures with inductive coupling," *Appl. Phys. Lett.* **78**, 498–500 (2001).
9. E. Plum, V. A. Fedotov, A. S. Schwanecke, N. I. Zheludev, and Y. Chen, "Giant optical gyrotropy due to electromagnetic coupling," *Appl. Phys. Lett.* **90**, 223,113 (2007).
10. C. Imhof and R. Zengerle, "Strong birefringence in left-handed metallic metamaterials," *Opt. Commun.* **280**, 213–216 (2007).
11. W. J. Padilla, A. J. Taylor, C. Highstrete, M. Lee, and R. D. Averitt, "Dynamical Electric and Magnetic Metamaterial Response at Terahertz Frequencies," *Phys. Rev. Lett.* **96**, 107,401 (2006).
12. H.-T. Chen, W. J. Padilla, J. M. O. Zide, A. C. Gossard, A. J. Taylor, and R. D. Averitt, "Active terahertz metamaterial devices," *Nature* **444**, 597–600 (2006).
13. V. D. Veselago, "The electrodynamics of substances with simultaneously negative values of ϵ and μ ," *Soviet Physics Uspekhi* **10**, 509–514 (1968).
14. D. R. Smith, W. J. Padilla, D. C. Vier, S. C. Nemat-Nasser, and S. Schultz, "Composite Medium with Simultaneously Negative Permeability and Permittivity," *Phys. Rev. Lett.* **84**, 4184–4187 (2000).
15. M. Gokkavas, K. Guven, I. Bulu, K. Aydin, R. S. Penciu, M. Kafesaki, C. M. Soukoulis, and E. Ozbay, "Experimental demonstration of a left-handed metamaterial operating at 100 GHz," *Phys. Rev. B* **73**, 193,103 (2006).
16. N. Katsarakis, G. Konstantinidis, A. Kostopoulos, R. S. Penciu, T. F. Gundogdu, M. Kafesaki, E. N. Economou, T. Koschny, and C. M. Soukoulis, "Magnetic response of split-ring resonators in the far-infrared frequency regime," *Opt. Lett.* **30**, 1348–1350 (2005).

17. H. O. Moser, B. D. F. Casse, O. Wilhelmi, and B. T. Saw, "Terahertz response of a microfabricated rod-splitting-resonator electromagnetic metamaterial," *Phys. Rev. Lett.* **94**, 63,901 (2005).
18. J. B. Pendry, A. J. Holden, D. J. Robbins, and W. J. Stewart, "Magnetism from Conductors and Enhanced Non-linear Phenomena," *IEEE Trans. Microwave Theory Tech.* **47**, 2075–2084 (1999).
19. J. B. Pendry, A. J. Holden, W. J. Stewart, and I. Youngs, "Extremely Low Frequency Plasmons in Metallic Mesostructures," *Phys. Rev. Lett.* **76**, 4773–4776 (1996).
20. V. M. Shalaev, W. Cai, U. K. Chettiar, H.-K. Yuan, A. K. Sarychev, V. P. Drachev, and A. V. Kildishev, "Negative index of refraction in optical metamaterials," *Opt. Lett.* **30**, 3356–3358 (2005).
21. G. Dolling, C. Enkrich, M. Wegener, J. F. Zhou, C. M. Soukoulis, and S. Linden, "Cut-wire pairs and plate pairs as magnetic atoms for optical metamaterials," *Opt. Lett.* **30**, 3198–3200 (2005).
22. S. Zhang, W. Fan, N. C. Panoiu, K. J. Malloy, R. M. Osgood, and S. R. J. Brueck, "Experimental Demonstration of Near-Infrared Negative-Index Metamaterials," *Phys. Rev. Lett.* **95**, 137,404 (2005).
23. G. Dolling, C. Enkrich, M. Wegener, C. M. Soukoulis, and S. Linden, "Simultaneous Negative Phase and Group Velocity of Light in a Metamaterial," *Science* **312**, 892–894 (2006).
24. G. Dolling, M. Wegener, C. M. Soukoulis, and S. Linden, "Negative-index metamaterial at 780 nm wavelength," *Opt. Lett.* **32**, 53–55 (2007).
25. G. Dolling, M. Wegener, and S. Linden, "Realization of a three-functional-layer negative-index photonic metamaterial," *Opt. Lett.* **32**, 551–553 (2007).
26. N. Liu, H. Guo, L. Fu, S. Kaiser, H. Schweizer, and H. Giessen, "Three-dimensional photonic metamaterials at optical frequencies," *Nat. Mater.* **7**, 31–37 (2008).
27. C. Imhof and R. Zengerle, "Pairs of metallic crosses as a left-handed metamaterial with improved polarization properties," *Opt. Express* **14**, 8257–8262 (2006).
28. K. Aydin, K. Guven, M. Kafesaki, L. Zhang, C. M. Soukoulis, and E. Ozbay, "Experimental observation of true left-handed transmission peaks in metamaterials," *Opt. Lett.* **29**, 2623–2625 (2004).
29. X. Chen, T. M. Grzegorzczak, B.-I. Wu, J. Pacheco, Jr., and J. A. Kong, "Robust method to retrieve the constitutive effective parameters of metamaterials," *Phys. Rev. E* **70**, 016,608 (2004).
30. R. A. Depine and A. Lakhtakia, "A new condition to identify isotropic dielectric-magnetic materials displaying negative phase velocity," *Microwave Opt. Technol. Lett.* **41**, 315–316 (2004).
31. J. Zhou, L. Zhang, G. Tuttle, T. Koschny, and C. M. Soukoulis, "Negative index materials using simple short wire pairs," *Phys. Rev. B* **73**, 041,101 (2006).
32. G. Dolling, C. Enkrich, M. Wegener, C. M. Soukoulis, and S. Linden, "Low-loss negative-index metamaterial at telecommunication wavelengths," *Opt. Lett.* **31**, 1800–1802 (2006).
33. R. A. Shelby, D. R. Smith, and S. Schultz, "Experimental Verification of a Negative Index of Refraction," *Science* **292**, 77–79 (2001).

1. Introduction

Electromagnetic metamaterials, composed of metallic elements which are smaller than the operating wavelength, have gained a lot of attraction during the last decade. The possibility of creating an effective medium with controllable permittivity and permeability makes this kind of materials very interesting for many applications [1–12]. From a scientific point of view media not naturally occurring are of interest, in particular those with a negative index of refraction [13, 14]. Since in such media the vectors of the electric and the magnetic field and the wave vector form a lefthanded coordinate system, these materials are also referred to as lefthanded materials. The most common design for lefthanded metamaterials in the terahertz regime [15–17] is a combination of split ring resonators [18] with thin metallic wires [19]. However, the resulting material is very sensitive to the polarization of the incident electromagnetic field. Moreover, to ensure optimal coupling to the resonant elements, the propagation direction of the electromagnetic waves has to be parallel to the plane of the split rings. Since for higher operating frequencies only planar structures can be fabricated by standard techniques, this requirement is equivalent to propagation parallel to the boundary between the metamaterial and the surrounding medium. Therefore, some new metamaterial concepts for waves propagating normal to the plane of the structures have been proposed and realized for the infrared and optical region [20–24]. The realization of bulk devices for frequencies beyond 200 GHz remains a big challenge. Recently, two different approaches have been made concerning the fabrication of multi-layer metamaterials [25, 26]. However, the fabrication process of the three-functional

layer fishnet-structure [25] includes a sensitive lift-off procedure and is limited to a small number of layers. In the second approach a lot of effort has to be made in order to get the optimal arrangement of the different layers because of the polarization dependent behavior of the used metastructures [26]. The ability to manufacture bulk metamaterials is an inevitable requirement for nearly all possible applications, like plane parallel lenses [1,2], cloaking and invisible materials [3–6], as well as the construction of polarization manipulating devices [7–10] and tunable metamaterials [11, 12].

2. Structure design and fabrication

To avoid the aforementioned problems, we have chosen a structure built up by pairs of metallic crosses which has been theoretically analyzed in the microwave regime [27]. A schematic drawing of four unit cells of the implemented structure with all geometrical data is shown in Fig. 1. The basic functionality of this structure is similar to that of the cut wire pair design [20]. The two perpendicular pairs of crossbars represent two independent sets of wire pairs. These wires act as small electrical dipoles which lead to a negative effective permittivity. Additionally, two opposing crossbars within one elementary cell form some kind of LC-resonance circuit, which can be excited by a magnetic flux through the area between the two wires. This mechanism drives the effective permeability to negative values. Therefore, if the frequency bands of the electric and the magnetic response overlap, a lefthanded behavior can be observed for a plane wave impinging perpendicularly to the cross plane. Due to the symmetry of the cross structure, this functionality is independent of the polarization of the wave.

The fabrication of a single layer of elementary cells of the cross pair structure is done in a multilayer process with alternating layers of BCB 3022-67 and copper and is illustrated in Fig. 2. The sequence starts with spinning two layers of BCB with an overall thickness of $25\ \mu\text{m}$ on a silicon substrate. After thermal curing in a vacuum oven at $300\ ^\circ\text{C}$ for about 5 h, the first $200\ \text{nm}$ thick layer of crosses is produced on top using standard UV-lithography techniques performed with an EVG 620 mask aligner. A microscope image of the resulting cross layer is shown in Fig. 1. After spinning and curing a $9.5\ \mu\text{m}$ thick intermediate layer of BCB the second layer of crosses is fabricated precisely above the first. Since strict alignment of the two single crosses within each elementary cell is necessary to ensure the functionality of the structure, we use alignment marks providing an accuracy in the order of $1\ \mu\text{m}$. The layer of elementary cells is completed by spinning and curing another two BCB layers with an overall thickness of $27\ \mu\text{m}$. The metallic structures are now completely embedded in films of BCB providing a

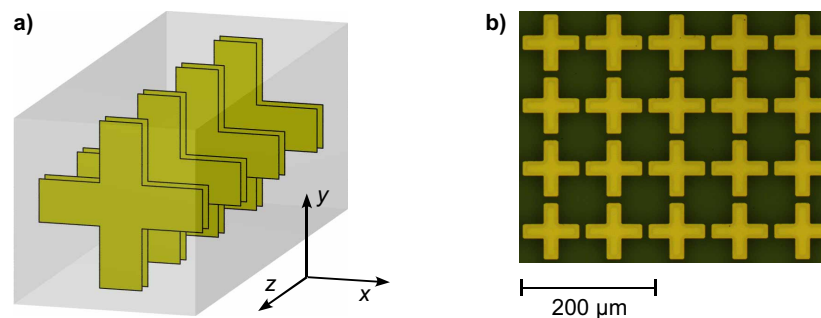


Fig. 1. The cross pair structure. a) Schematic drawing of four unit cells with lattice constants $a_x = a_y = 90\ \mu\text{m}$, $a_z = 62\ \mu\text{m}$, length of a crossbar = $81\ \mu\text{m}$, width of a crossbar = $21\ \mu\text{m}$, separation of a cross pair = $9.5\ \mu\text{m}$. b) Microscope image of a single cross layer.

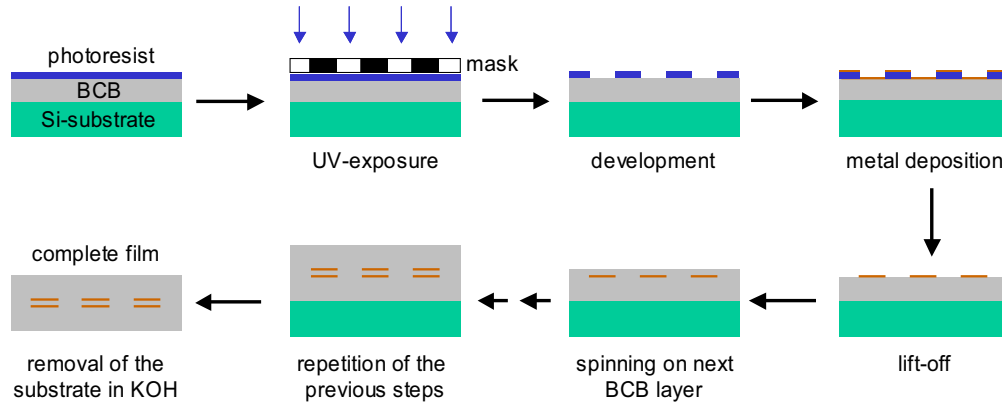


Fig. 2. Illustration of the fabrication process of one layer of cross pairs embedded in BCB.

homogeneous background as well as symmetry along the direction of propagation. On top of some samples the whole procedure is repeated to obtain films with two layers of cross pairs. The films are then removed from the substrate in a 30% solution of KOH. Furthermore, we prepared metamaterials with three and four layers of cross pairs by simply stacking a two-layer film on top of a one- and two-layer film, respectively.

3. Experimental results and numerical simulations

We analyzed the transmission properties of the metamaterials by a standard THz time domain spectroscopy system, performed with linearly polarized waves and a frequency resolution of 5 GHz. The transmission spectra for different layers of cross pairs are measured and normalized by a reference spectrum without sample. The resulting amplitude transmittance spectra are compared with numerical simulations, which are performed with a commercially available time domain solver for the Maxwell equations. The required dielectric parameters of BCB have been determined by previous measurements on bulk BCB in the same frequency range, yielding a dielectric constant $\epsilon = 2.67$ and a loss parameter $\tan \delta = 0.012$. To improve the accuracy of the simulation algorithm the dielectric dispersion of copper is included by a Drude model.

The resulting curves are shown in Fig. 3 and reveal a well-defined transmission peak at about 1.02 THz in the middle of a broad stop band. As the number of layers is increased, the contrast between the transmission band and the stop band grows. The measured spectra are not affected by the orientation of the metamaterial sample with respect to the polarization direction of the THz waves. From the preliminary considerations, it is expected that the observed peak is lefthanded. In order to confirm this prediction we compare the measurements of a one layer thick cross-pair metamaterial with transmission data of a structure fabricated with only one cross per elementary cell. In this modified design the magnetically resonant LC-circuit is no longer present and only the electric response of the structure can have an effect [28]. The corresponding measurements in Fig. 4 show that the modified structure leads to a termination of the transmission peak. The unaffected stop band thus represents the region where the electric resonance of the structure causes a negative permittivity. Since transmission can only take place if both the permittivity and the permeability are negative, this experimentally indicates that the observed transmission peak at 1.02 THz is lefthanded [28].

Furthermore, as can be seen in Fig. 3, there is no direct influence from the mechanical stacking process, which is performed without any control of the alignment between the individual

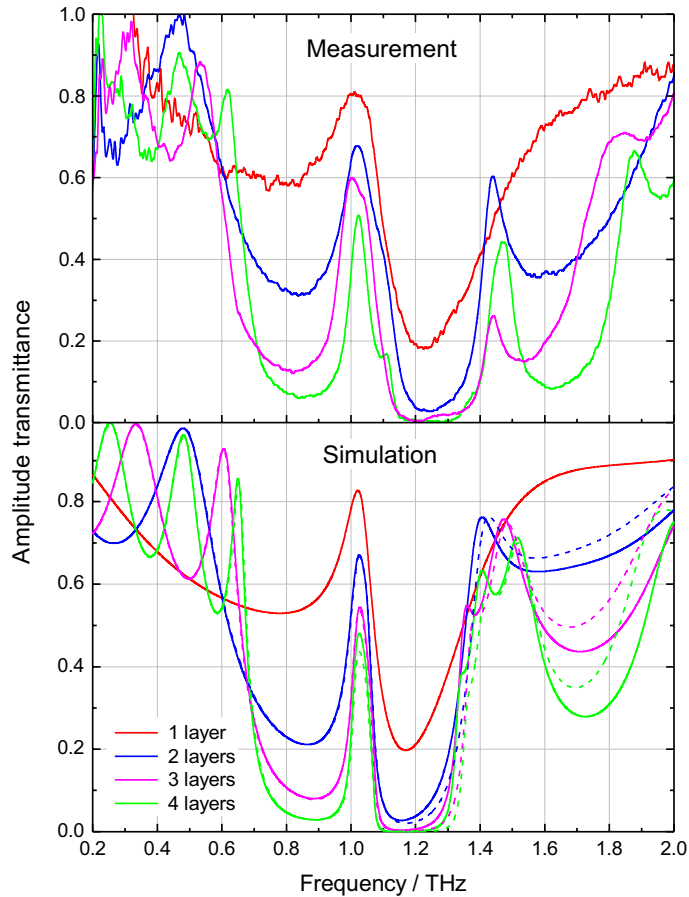


Fig. 3. Amplitude transmittance of metamaterial slabs consisting of 1–4 layers of cross pairs. Comparison of the measured spectra (upper figure) with directly simulated curves (lower figure, solid lines) and curves derived from the transmission matrix of a one-layer structure under the assumption of independent layers (dashed lines).

films, on the transmission properties of the metamaterial. The spectral position of the transmission peak remains centered around 1.02 THz and the agreement with the numerical simulations, where all layers of cross pairs are perfectly aligned, is very good. To numerically verify the statement that the relative alignment of consecutive layers is not crucial, we compare the simulated amplitude transmittance of a metamaterial slab consisting of 2–4 layers with the results derived from the transmission matrix T of a simulated one-layer structure. If the layers can be treated as independent the transmission matrix $T(n)$ of an n -layer structure is given by

$$T(n) = T^n \quad (1)$$

The resulting curves are plotted in Fig. 3 as dashed lines. In the relevant frequency region below 1.5 THz there is nearly no difference between the directly simulated curves and the curves calculated under the assumption of independent layers. In particular, since the single cross pair layers are inherently independent of the polarization, the validity of Eq. (1) implies that the composite medium is insensitive of both the relative position and orientation of the individual

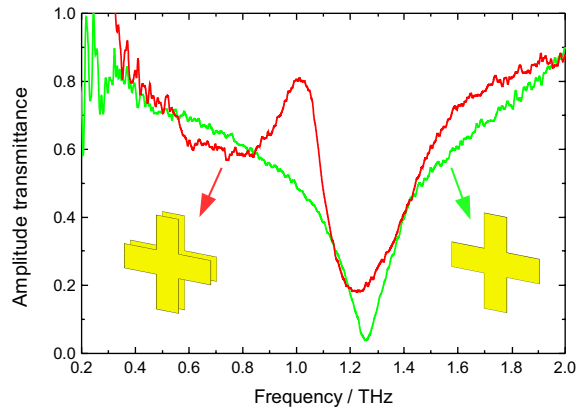


Fig. 4. Comparison of the amplitude transmittance between the cross pair and the single cross design for one layer of elementary cells.

layers. Thus, single fabricated films can be simply stacked on top of another to increase thickness and to obtain a real bulk metamaterial. No effort for the alignment of the individual films is necessary. This is a significant simplification of the fabrication process in comparison to existing multi-layer metamaterials [25, 26]. Since BCB exhibits excellent planarization properties, the useful number of layers in our design is only limited by the overall absorption of BCB.

The good agreement of the measured transmission spectra with the simulated curves evidences the high accuracy of the used simulation model. Therefore, the field simulation can be used to further work out reliable characteristics of our metamaterial. In particular, the simulation of the phase progression of a plane wave while propagating through the metamaterial will further consolidate the prediction that the observed transmission peak is lefthanded. This is shown exemplarily for a frequency of 1.03 THz in Fig. 5. It can be seen that the average slope of the phase changes its sign inside the metamaterial. This confirms that the phase velocity and thus the refractive index are negative within the observed transmission band.

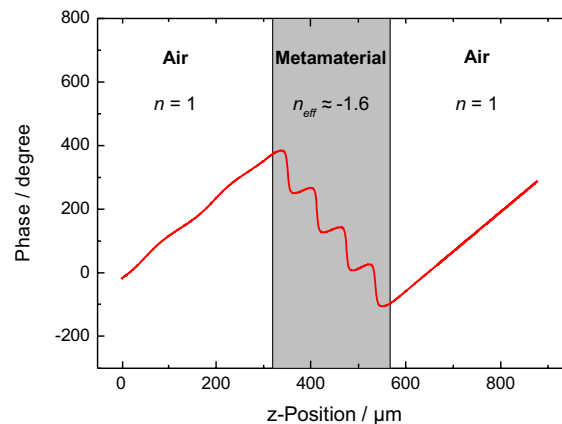


Fig. 5. Simulated phase of the electric field along a path through the metamaterial for a plane wave at 1.03 THz.

4. Parameter retrieval

For a complete quantitative characterization of the electromagnetic properties of our metamaterial we apply a retrieval procedure [29] to calculate the effective refractive index n and the wave impedance z from the simulated reflection and transmission data. The effective permittivity ϵ and permeability μ are then directly obtained by $\epsilon = n/z$ and $\mu = nz$. The retrieval procedure was carried out with respect to a one-layer cross pair structure. However, the use of multi-layer simulation data shows no significant effect on the retrieved parameters. The resulting effective parameters are plotted in Fig. 6, where $(\cdot)'$ and $(\cdot)''$ denote the real and imaginary part, respectively.

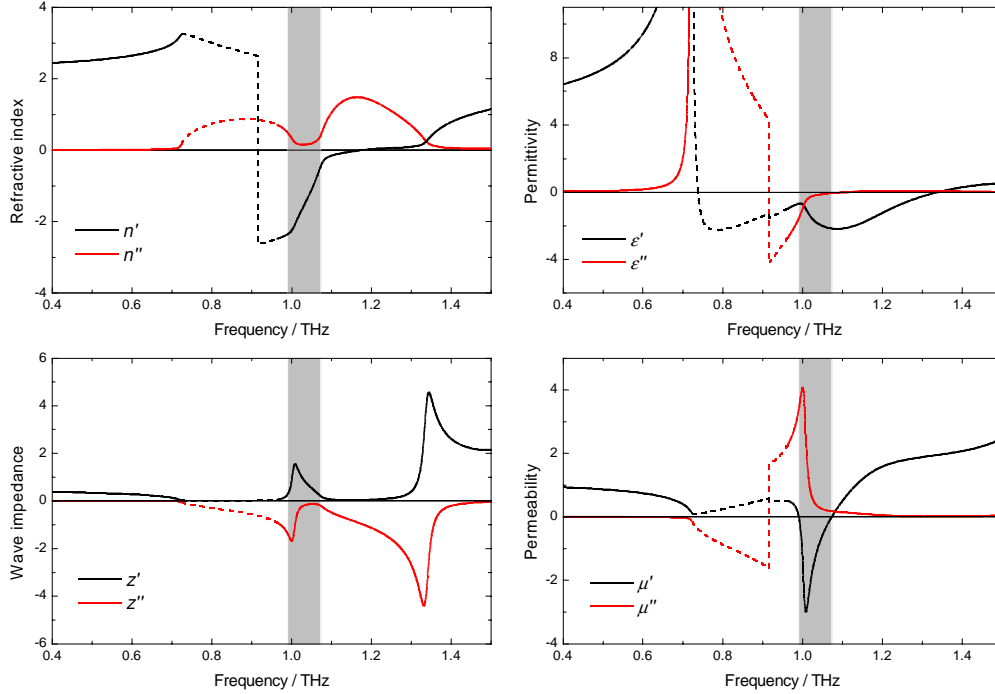


Fig. 6. Effective material parameters retrieved from the simulated reflection and transmission data. $(\cdot)'$ and $(\cdot)''$ denote the real and imaginary part, respectively. The lefthanded transmission band is shaded. The dashed parts of the curves mark the regions where the half-wavelength inside the medium is smaller than the lattice constant a_z and the calculated effective parameters are not expected to be reliable.

In agreement with the experimental results, there is a narrow band with negative μ' lying in a relatively broad band with negative ϵ' . The frequency band where the general condition for negative refraction [30]

$$\epsilon'|\mu| + \mu'|\epsilon| < 0$$

is satisfied, is located between 0.96 and 1.17 THz. However, because of the high losses n'' at the borders of this region, it is more appropriate to apply the stricter condition

$$\epsilon' < 0, \mu' < 0$$

for the definition of the lefthanded band, since here the losses remain small and transmission

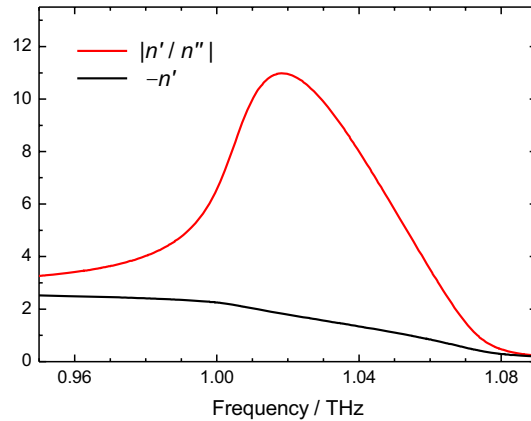


Fig. 7. Figure of merit $|n'/n''|$ for the frequency region with negative refractive index.

can take place [31]. This band is located between 0.99 and 1.07 THz and coincides with the measured transmission peak.

With regard to possible applications, a well-established measure of the strength of the negative refraction with respect to the losses is the figure of merit

$$F = \left| \frac{n'}{n''} \right|$$

As shown in Fig. 7 this value reaches a maximum of $F = 11.0$ at 1.02 THz and is $F = 4.8$ for $n' = -1$. This value is quite high compared with other structures used in this frequency range. For the classic split ring and wire structure operating at 100 GHz a maximum value of $F = 6$ is reported [15]. In the optical range the largest figure of merit $F = 3$ was obtained with a fishnet structure at 1.4 μm wavelength [32].

5. Conclusion

We have demonstrated a lefthanded bulk metamaterial operating in the THz frequency range. The presented structure operates at normal incidence and is independent of the polarization. We have used simple multilayer techniques to embed the functional metallic structures completely in BCB, which allows the removal of the silicon substrate after processing. Due to the simple structure design and the polarization independence, the lifted structures can be mechanically stacked on top of another to further increase the thickness and obtain a real bulk metamaterial. The observed transmission spectrum is in good agreement with numerical simulations and evidences a lefthanded transmission band at about 1 THz with a high figure of merit.

With regard to possible applications, the operating frequency and transmittance of the metamaterial can be adjusted by modifying the structure design. A polarization sensitive behavior can be included by varying geometric parameters like the length or the width of one pair of crossbars with respect to the other pair [10]. The metamaterial thus offers a wide variety of applications in the THz frequency range, like wave plates, band pass filters, beam steerers or aberration-free, plane parallel lenses. From a scientific point of view, the presented metamaterial allows a direct verification of the negative refraction based on Snell's law. Such fundamental experiments have been realized in the microwave regime [33] and a realization at higher frequencies is a target of further research.

Acknowledgment

We would like to acknowledge support from the Center for Nanostructure Technology and Biomolecular Technology of Kaiserslautern, Germany and thank Dr. Sandra Wolff for continuous help and valuable discussions.